Journal of Materials Chemistry A

First principles study of dopant solubility and defect chemistry in $LiCoO_2$

Journal:	*Journal of Materials Chemistry A*
Manuscript ID:	TA-ART-03-2014-001443.R1
Article Type:	Paper
Date Submitted by the Author:	21-Apr-2014
Complete List of Authors:	Koyama, Yukinori; Kyoto University, Office of Society-Academia Collaboration for Innovation Arai, Hajime; Kyoto University, Office of Society-Academia Collaboration for Innovation Tanaka, Isao; Kyoto University, Department of Materials Science and Engineering Uchimoto, Yoshiharu; Kyoto University, Graduate School of Human and Environment Studies Ogumi, Z; Kyoto University, Office of Society-Academia Collaboration for Innovation

Cite this: DOI: 10.1039/c0xx00000x

www.rsc.org/xxxxxx

FULL PAPER

First principles study of dopant solubility and defect chemistry in $LiCoO_2$

Yukinori Koyama,*[a] Hajime Arai,[a] Isao Tanaka,[b] Yoshiharu Uchimoto[c] and Zempachi Ogumi[a]

Received (in XXX, XXX) Xth XXXXXXXXX 20XX, Accepted Xth XXXXXXXXX 20XX

DOI: 10.1039/b000000x

Doping and alloying are extensively applied to electrode active materials to improve performance of lithium-ion batteries. Thus, defect formation energy and equilibrium concentrations of doped ions in $LiCoO_2$ are estimated as extrinsic point defects, as well as those of the native defects, using first-principles calculations. Na, K, Rb, Mg, Ca, Sr, Zn, Al, Ga, In, Sc, Y, Zr and Nb are selected as the dopants with a variety of valences and ionic radii. Dopants having solubility higher than 1 % are Al and Ga for the Co site, and Na and Zn for the Li site at 1100 K and 0.2 atm oxygen pressure without significant increase in lithium deficiency. Mg shows solubility of about 0.5 % at both the sites, and the preferential occupation site depends on conditions: the Co site at oxidative conditions, whereas the Li site at reductive conditions. The estimated dopant solubility indicates that the valences of the dopants are the predominant factor for the occupation sites, whereas the ionic radii have a significant effect on the solubility. The dopant solubility and defect concentrations strongly depend on the chemical potentials. Therefore, appropriate ratio of starting materials that provides the desirable chemical potentials is necessary to achieve the balance of the high dopant solubility and the low lithium deficiency. The present calculation based on the first-principles calculations can provide quantitative information about the balance of the defects and also about the proper synthetic and post-synthetic conditions.

Introduction

Modification of electrode active materials is often carried out to improve performance of lithium-ion batteries. Extensive studies have been reported on doping and alloying to the electrode active materials. Tukamoto and West reported comprehensive synthesis of doped $Li(M_{0.05}Co_{0.95})O_2$ with divalent and higher-valent dopants to enhance electronic conductivity, and they obtained single-phase products only with M = Mg, Cr, Ni, B, Al and Ga.[1] Al,[2-4] Ga[5,6] and Mg[1,7-10] are often doped to layered active materials, *e.g.*, $LiCoO_2$ and $LiNiO_2$, to stabilize the layered structure, suppress dissolution of the transition metals, improve thermal stability, *etc*. Although Tukamoto and West reported observation of impurity phases for Zr doping, several trials of the Zr doping and scattered results are reported: some groups reported that the Zr doping improves cycling performance,[9,11] whereas other groups reported that Zr is insoluble to $LiCoO_2$.[1,12,13] As for monovalent dopants, Bludská *et al.* reported synthesis of Na-doped $LiCoO_2$.[14] But the Na solubility is not clear, since the reported lattice parameters are constant against the Na composition. Holzapfel *et al.* reported that the solubility limit of Na to $LiNiO_2$ was 6 %, and they found simultaneous substitution of Ni for Li.[15] For proper control of doping/alloying, information about the doped ions such as the occupation sites and the solubility limits is essential. However, experimental determination on whether the dopants are soluble or insoluble is generally based on observation of other phases. Thus, one has difficulty of the determination, particularly with low solubility, leading to limited and qualitative information on the doping. Moreover, the doped ions are extrinsic point defects for the electrode active materials, and it is well known that the point defects have a significant influence on various properties of the active materials.[16-20] Therefore, it is of importance to consider effect of the doping upon chemistry of native (intrinsic) defects in the active materials.

Surface coating is another commonly used modification applied to the electrode active materials in order to improve the capacity retention and other performance.[21-28] Some reports show that coating materials may react with the electrode active materials during the coating processes, resulting in unexpected doping of the coating species to the active materials.[21,26] Therefore, chemistry of doping in the electrode active materials is of great importance to design appropriate modification of the electrode active materials.

First-principles density functional theory (DFT) calculations have been performed to investigate the doping and alloying to the electrode active materials for the lithium-ion batteries.[29-39] Most of these studies focus on solid-solution systems, and molar ratios of the added species are relatively high, typically 25–50 %.[29-35] On the other hand, some studies investigate dilute doped ions like

point defects by a concentration of 3–8 % in supercells, although the occupation sites and concentrations are given *a priori*.[36-38] For designing the modification to the electrode active materials, the question is the solubility limit of the dopants on individual sites with respect to chemical conditions for synthetic and modification processes such as temperature and oxygen partial pressure.

We herein report the defect formation energy and equilibrium concentration of doped ions in $LiCoO_2$ estimated as extrinsic point defects, as well as those of the native defects. We select Na, K, Rb, Mg, Ca, Sr, Zn, Al, Ga, In, Sc, Y, Zr and Nb as the dopants. The set of the dopants has a variety of valences and ionic radii and includes what is not reported to be soluble to $LiCoO_2$, to discuss the major factor that determines the solubility and the occupation sites. Here we examine only a few transition metals with fixed valences, namely Zr^{4+} and Nb^{5+}, because the valences of transition metals are often indefinite. We discuss the effect of the chemical conditions of temperature and chemical potentials on the dopant solubility as well as that on the concentrations of the native defects, particularly lithium-deficient defects. High lithium deficiency is very likely undesirable for the practical use as the electrode active materials, considering that $LiNiO_2$ with high lithium deficiency shows poor reversible capacity.[17,18] We also give a guide to appropriate conditions with respect to balance of increase in the dopant solubility and suppression of the lithium deficiency. Finally we discuss the major factor that determines the solubility and the occupation sites of the dopants from the point of view of solid-state chemistry.

Computational details

Dopant and defect models

We have previously reported the formation energy and equilibrium concentration of native defects in layered lithium transition-metal oxides using first-principles calculations.[40,41] For the estimation of the dopant solubility, the calculation scheme is extended in the doped ions as the extrinsic defects as follows. The dopants examined in this study are Na, K, Rb, Mg, Ca, Sr, Zn, Al, Ga, In, Sc, Y, Zr and Nb. The doped ions substitute for both Li and Co, and they are respectively denoted as M_{Li} and M_{Co} on Kröger–Vink notation, where M is the doped species. Vacancies (V_{Li}, V_{Co} and V_O), interstitial cations (Li_i and Co_i) at the tetrahedral site in the Li layers, antisite cations (Co_{Li} and Li_{Co}), and electronic defects (e^- and h^+) as small polarons are examined as the native defects. Several charges were examined from the neutral to the formal values estimated from the regular oxidation states for individual defects. As the defects may be complexes of other defects with different charges and coupled electronic defects, many possible combinations of the defects and their arrangements were first examined for each nominal charge, and then the defect having the lowest energy was selected for detailed calculations.

Defect formation energy and equilibrium concentration

Formation energy of defect X at site A in charge state q (X_A^q) is defined as

$$\Delta_f E(X_A^q) = E(X_A^q) - E(\text{bulk}) - \Sigma_i \Delta n_i \mu_i + q \varepsilon_F, \quad (1)$$

where $E(X_A^q)$ and E(bulk) are the energies of the supercells obtained by first-principles calculations with and without the defect, respectively. Δn_i is the change in the number of atoms of species i, which has been added ($\Delta n_i > 0$) or removed ($\Delta n_i < 0$). μ_i is the atomic chemical potential of species i. ε_F is Fermi energy. Note that energies in Eq. 1 are, in principle, Gibbs free energies. However, the entropy and volume terms can be disregarded for solid phases. Under a thermal equilibrium condition, concentration of defect X_A^q at temperature T can be obtained as

$$C(X_A^q) = C(A_A)\, N_{\text{config}} \exp(-\Delta_f E(X_A^q) / k_B T), \quad (2)$$

where $C(A_A)$ is the concentration of site A without any defect. N_{config} is the number of equivalent configurations per site, and it is assumed to be 1 for all the defects in this study for simplicity. k_B is the Boltzmann constant.

To represent a thermal equilibrium system of M-doped $LiCoO_2$, one internal parameter (Fermi energy, ε_F) and five external parameters, typically temperature (T) and atomic chemical potentials of the constituent species (μ_{Li}, μ_{Co}, μ_O and μ_M), are necessary to be specified. Fermi energy was determined so that the system satisfied charge neutrality. The existence of $LiCoO_2$ as a thermodynamically stable phase requires a relationship among the chemical potentials as

$$\mu_{Li} + \mu_{Co} + 2\,\mu_O = E(LiCoO_2), \quad (3)$$

where $E(LiCoO_2)$ is the energy of $LiCoO_2$ obtained by first-principles calculations. In addition to $LiCoO_2$, there are many substances in the Li–Co–M–O system, *e.g.*, elementary substances, Li_2O, and possibly complex oxides of M with Li and/or Co. These substances potentially compete with $LiCoO_2$ for the thermodynamic stability. In this study, $LiCoO_2$ is supposed to be the thermodynamically stable phase, and the competing phases are unstable or coexistent with $LiCoO_2$. This imposes another constraint on the stability region of $LiCoO_2$ in terms of the chemical potentials as

$$a\,\mu_{Li} + b\,\mu_{Co} + c\,\mu_M + d\,\mu_O \le E(Li_aCo_bM_cO_d) \quad (4)$$

for any other phase of $Li_aCo_bM_cO_d$. The stability region of $LiCoO_2$ is then defined after taking account of the constraints imposed by all possible competing phases. The stability region of $LiCoO_2$ generally forms a polyhedron in a space of the chemical potentials, and the limits of chemical potentials imposed by the competing phases correspond to boundaries of the polyhedron.

This study supposes synthetic and heat-treatment processes for $LiCoO_2$ to discuss the doping. $LiCoO_2$ is generally synthesized at temperatures of 800–900 °C in air.[42] Doped ions are dissolved into $LiCoO_2$, and native defects are formed at the high temperatures. A part of them remain in the samples even after cooling to room temperature, owing to their slow diffusion at low temperatures. Thus, temperature is set in a range of 900–1300 K, and the defect concentrations are mainly discussed at 1100 K. Atomic chemical potential of O is estimated as

$$\mu_O = 1/2\,(E_{O_2}^{\text{DFT}} + (G_{O_2}^0(T) - G_{O_2}^0(0\text{ K})) + k_B T \ln(P_{O2}/P^0)), \quad (5)$$

where $E_{O_2}^{\text{DFT}}$ is the energy of an O_2 molecule obtained by first-principles calculations. $G_{O_2}^0$ is the Gibbs free energy of the gaseous O_2 phase under the standard pressure P^0 as a function of

temperature, which is estimated assuming the ideal gas based on experimental results.[43] The partial pressure of O_2, P_{O2}, is fixed to be 0.2 atm. The conditions of the synthetic and heat-treatment processes are usually specified by temperature, gas condition, and ratio of starting materials. The chemical potentials of the metal species are indirectly controlled. At the solubility limit of the dopants, residuals of excess species are observed as secondary phases. As this study focuses on the solubility limit, the chemical potentials of the metal species are set at the limits of the stability region of $LiCoO_2$ coexisting with specified phases. Three-phase coexistence conditions are typically selected so that the chemical potentials are uniquely defined, as detailed later.

First-principles calculation

The defect energies were calculated using 144-atom ($Li_{36}Co_{36}O_{72}$) supercells constructed by the expansion of the α-$NaFeO_2$-type unit cell by $2\sqrt{3} \times 2\sqrt{3}$ in the *ab* plane. Single defects were individually introduced into the supercells. Lattice parameters were fixed at those of pristine $LiCoO_2$ obtained by first-principles calculations (a = 2.832 Å and c = 14.20 Å).[40] Atomic positions were optimized until the residual forces became smaller than 0.02 eV $Å^{-1}$. The electrostatic potentials of the charged supercells were corrected by the "potential alignment" method, *i.e.*, the electrostatic potentials at the farthest ions from the defects are adjusted to those in the pristine crystal.[40,41,44-46]

The first-principles calculations were performed using the plane-wave basis projected-augmented-wave (PAW) method implemented in the Vienna *Ab initio* Simulation Package (VASP) code.[47-49] The plane-wave basis set was determined with a cutoff energy of 500 eV. Integral in the reciprocal space was evaluated by the Gaussian smearing technique with a smearing parameter of 0.1 eV and a 2 × 2 × 1 mesh. Spin polarization was considered. The exchange-correlation interaction was treated by the generalized gradient approximation (GGA).[50] The Hubbard model correction[51] was applied to Co-3*d* states with a U parameter of 5 eV,[40] whereas the correction was not used for the other species including Zr and Nb.

Results and discussion

Doping of Al

Various complex oxides of Al with Li and Co are known. These complex oxides impose limits on the stability region of $LiCoO_2$. Figure 1 illustrates the stability region of $LiCoO_2$ projected on a space of Li and Al chemical potentials at a temperature of 1100 K and an O_2 pressure of 0.2 atm. As polymorphs are known for Li_5AlO_4 and $LiAlO_2$, the high-temperature forms of β-Li5AlO_4 and γ-$LiAlO_2$ are selected as the possible competing phases. $CoAl_2O_4$ shows disordering between Co and Al ions at the tetrahedral and octahedral sites of the spinel structure, but the regular spinel structure is assumed. Definition of defect formation energy, Eq. 1, suggests that higher Al chemical potential is desirable to reduce the formation energies of doped Al, *i.e.*, Al_{Li} and Al_{Co}, and thus to increase Al solubility in $LiCoO_2$. It also suggests that higher Li chemical potential is desirable to increase the formation energies of lithium-deficient defects, *e.g.*, Co_{Li} and V_{Li}, and thus to suppress the lithium deficiency. Figure 1, however, shows that the maximum Al chemical potential and the maximum Li one are incompatible in the stability region of $LiCoO_2$. Therefore, defect formation energies are evaluated at several limit conditions of the stability region of $LiCoO_2$, where $LiCoO_2$ coexists with other phases.

Figure 2 illustrates defect formation energies at conditions A–C in Fig. 1 as a function of Fermi energy. Fermi energy is measured from the valence-band maximum (VBM), which corresponds to zero formation energy of h^+. Conduction-band minimum (CBM), which corresponds to zero formation energy of e^-, is located at 1.36 eV above.[40] Defects having positive relative-charges, *e.g.*, Co_{Li}^+, Co_{Li}^{2+}, V_O^{2+} and h^+, show small formation energies near the VBM, whereas e^- does a small formation energy near the CBM. Assuming that the system follows the charge neutrality, Fermi energy exists close to the crossing point of Co_{Li}^+ and e^-. Since Al_{Co}^0 has the zero relative charge, its formation energy is independent from Fermi energy: 0.23 eV at condition A, where $LiCoO_2$ coexists with Li_2O and Li_5AlO_4, and almost 0 eV at conditions B (with Li_5AlO_4 and $LiAlO_2$) and C (with $LiAlO_2$ and $CoAl_2O_4$). Although the formation energy of Al_{Li}^{2+} is small near the VBM, it becomes larger than 2 eV at the charge neutral condition. Al_{Li}^0, which is a complex defect of Al_{Li}^{2+} with two associated e^- at the nearest neighboring Co ions, shows smaller formation energy at the charge neutral condition than Al_{Li}^{2+}, but the formation energy is 1.42 eV (at condition C) or larger. The large formation energies of the series of Al_{Li} suggest that Al does not substitute for Li in $LiCoO_2$.

To search for conditions with low formation energy of doped Al and high formation energy of the lithium-deficient defects, the defect formation energies under the charge neutral condition are evaluated along the boundary of the stability region of $LiCoO_2$. Figure 3 illustrates the defect formation energies and chemical potentials of Li, Co and Al along conditions X–A–B–C–Y in Fig. 1. From condition X to B through A, the formation energy of Al_{Co}^0 monotonically decreases as Al chemical potential increases. In contrast, the formation energy is constant against the change in Al chemical potential in the range of conditions B–C. This is because the coexistence of $LiCoO_2$ with $LiAlO_2$ leads to increase in Al and Co chemical potentials and decrease in Li one by the same amount from condition B to C. Therefore, the change in Al chemical potential is canceled out in the formation energy of Al_{Co}^0. Decrease in Li chemical potential from condition A to Y leads to the inverse increase in Co chemical potential. This results in smaller formation energies of the lithium-deficient defects, *e.g.*, Co_{Li}^0, Co_{Li}^+ and V_{Li}^-. The different decrease in the formation energy between Co_{Li}^0 and Co_{Li}^+ results from the change in Fermi energy, which indirectly depends on the chemical potentials through the defect concentrations under the charge neutral condition. Smaller formation energy of Al_{Co}^0 is practically associated with smaller formation energies of the lithium-deficient defects. Estimation of the defect concentrations is, therefore, of importance to find proper conditions for the Al doping.

Figures 4(a)–(c) respectively illustrate equilibrium defect concentrations in Al-doped $LiCoO_2$ at conditions A–C in Fig. 1 as a function of temperature. Figure 4(d) illustrates equilibrium defect concentrations in undoped $LiCoO_2$ coexisting with Li_2O[40] for comparison. The concentrations in the figure are the totals for each type of defects summed over all possible charges. At condition A, where $LiCoO_2$ coexists with Li_2O and Li_5AlO_4, the

concentration of Al_{Co} is estimated to be 8 % at 1100 K. On the other hand, the concentration of Al_{Li}, which is total of Al_{Li}^{0}, Al_{Li}^{+} and Al_{Li}^{2+}, is as low as 10^{-10}. As Al is a trivalent species the same as Co in $LiCoO_2$, the Al substitution for Co has little effect on the equilibrium concentrations of the native defects in $LiCoO_2$. At condition B, where $LiCoO_2$ coexists with Li_5AlO_4 and $LiAlO_2$, the concentration of Al_{Co} is estimated to be about 50 % at 1100 K. The concentration of Al_{Co} exhibits little dependence on temperature in the range of the usual synthetic conditions. Because of lower Li chemical potential and higher Co one than those at condition A, the concentrations of the lithium-deficient defects, *i.e.*, Co_{Li} and V_{Li}, become higher. However, the actual increases in the concentrations are insignificant as shown in Fig. 4(b); the concentration of Co_{Li} is still less than 1 % and that of V_{Li} is 10^{-6} at 1100 K. At the conditions where $LiCoO_2$ coexists with $LiAlO_2$, the formation energy of Al_{Co}^{0} is constant as shown in Fig. 3, and thus the defect concentration is also almost the same against the conditions as shown in Figs. 4(b) and (c). On the other hand, lower Li chemical potential and higher Co one at condition C than those at condition B lead to higher concentrations of the lithium-deficient defects: 6 % of Co_{Li} and 10^{-4} of V_{Li} at 1100 K.

Among the three examined conditions, condition B, coexistence of $LiCoO_2$ with Li_5AlO_4 and $LiAlO_2$, is the best with respect to balance of the high Al solubility and the low lithium deficiency. As Al substitutes for Co, condition B can be rewritten as a nominal composition of $Li(Al_xCo_{1-x})O_2$ with a small amount of excess Li. The high Al solubility in $LiCoO_2$ is already known by experiments ($x \sim 0.6$)[26] and also predicted by first-principles calculations ($x \sim 0.75$).[30] The high solubility suggested in the present study is in good agreement with the literature. Since mutual interaction among the doped ions and defects is disregarded in this study, there might be a lack of accuracy in the estimated defect concentrations, particularly in the case of very high concentrations. As compared with condition B, condition A can be interpreted as that excess Li is too much and it reacts with Al, leading to low Al chemical potential. This results in suppression of the Al solubility in $LiCoO_2$. On the other hand, condition C corresponds to the Al-rich and Li-poor condition. The estimated concentration of Co_{Li} of 6 % may be undesirably high for the practical use as the electrode active materials, considering that $LiNiO_2$ with high concentration of Ni ions in the Li layers shows poor reversible capacity.[17,18] To achieve the balance of the high Al solubility and the low lithium deficiency, proper ratio of the metal species is necessary: too much excess Li suppresses the Al solubility, whereas excess Al causes the lithium deficiency. The present estimation scheme based on the first-principles calculations can provide quantitative information about the balance of the defects and also about the proper conditions. This information is valuable not only for designing the synthetic processes but also for judging the appropriateness of the post-synthetic processes, *e.g.*, heat treatment for surface modification. Al_2O_3 coating is often applied to the electrode active materials.[23,26,28] The present calculation suggests that the surface of $LiCoO_2$ could react with coated Al_2O_3, resulting in the unexpected Al doping to $LiCoO_2$ and the increase in the lithium-deficient defects near the surface. The unexpected Al doping is already observed by experiments.[26]

Doping of other trivalent metals: Ga, Sc, In and Y

Ga forms complex oxides with Li and Co similar to Al, and the stability region of $LiCoO_2$ in Li and Ga chemical potentials is also similar. Equilibrium defect concentrations are evaluated at the equivalent conditions to the Al doping. Figure 5(a) illustrates the equilibrium defect concentrations in Ga-doped $LiCoO_2$ as a function of temperature, when $LiCoO_2$ coexists with Li_5GaO_4 and $LiGaO_2$. Ga preferentially substitutes for Co, and the concentration of Ga_{Co} is 2 % at 1100 K with small temperature dependence. It is reported that Ga is soluble by 5–10 % as $Li(Ga_xCo_{1-x})O_2$,[1,5] and the present calculation is comparable with the experiments. The concentrations of the lithium-deficient defects are slightly increased as compared with undoped $LiCoO_2$, but they are still less than 1 %. Too much excess Li, *e.g.*, coexisting with Li_2O and Li_5GaO_4, suppresses the Ga solubility in $LiCoO_2$, whereas excess Ga, *e.g.*, coexisting with $LiGaO_2$ and $CoGa_2O_4$, leads to the high lithium deficiency. The tendencies of the solubility and the lithium deficiency with respect to the coexisting phases are qualitatively the same as that for the Al doping.

Tukamoto and West reported that single-phase products of $Li(M_{0.05}Co_{0.95})O_2$ were obtained with M = Al and Ga, while impurity phases of $LiMO_2$ were observed with M = Sc, In and Y.[1] The later three species form complex oxides of $LiMO_2$, but not Li_5MO_4. Therefore, the equilibrium defect concentrations are estimated at conditions where $LiCoO_2$ coexists with Li_2O and $LiMO_2$. Figure 5(b) illustrates the equilibrium defect concentrations in Sc-doped $LiCoO_2$ as a function of temperature. The equilibrium concentration of Sc_{Co} is about 0.1 % at 1100 K, and that of Sc_{Li} is 10^{-7}. This suggests that Sc preferentially substitutes for Co rather than Li, although the solubility is low. Even under Sc-rich condition, *i.e.*, coexisting with $LiScO_2$ and Sc_2O_3, the concentration of Sc_{Co} is similar to that at the coexisting condition with Li_2O and $LiScO_2$. This is because the increase in Sc chemical potential is cancelled out by the increase in Co one when $LiCoO_2$ coexists with $LiScO_2$, which is analogous to the $LiCoO_2$ and $LiAlO_2$ coexistence. Instead, the concentrations of the lithium-deficient defects are significantly increased; the concentration of Co_{Li} becomes 40 % at 1100 K. In also substitutes for Co rather than Li. But the equilibrium concentration of In_{Co} is 10^{-6} when $LiCoO_2$ coexists with Li_2O and $LiInO_2$ at 1100 K. This suggests that In is almost insoluble in $LiCoO_2$. Estimated concentrations of Y_{Li} and Y_{Co} are as low as 10^{-10} at 1100 K at the condition where $LiCoO_2$ coexists with Li_2O and $LiYO_2$, indicating that Y is also insoluble in $LiCoO_2$. The low solubility of these trivalent dopants estimated in the present study is in good agreement with the literature.[1]

Doping of monovalent metals: Na, K and Rb

There are many known Na–Co oxides with and without Li. Energies of these oxides are calculated, and $Li_3Na_2CoO_4$ and $NaCoO_2$ are found to be stable phases coexisting with $LiCoO_2$. Figure 6(a) illustrates the stability region of Na-doped $LiCoO_2$ projected on a space of Li and Na chemical potentials at a temperature of 1100 K. Similar to the Al case, the maximum Li chemical potential and the maximum Na one are incompatible in Na-doped $LiCoO_2$. Therefore, equilibrium defect concentrations are evaluated at three-phase coexistence conditions, where

$LiCoO_2$ coexists with Li_2O and $Li_3Na_2CoO_4$ as denoted by condition A in Fig. 6(a), and with $Li_3Na_2CoO_4$ and $NaCoO_2$ as denoted by condition B. Figure 6(b) illustrates the equilibrium defect concentrations at condition A. The equilibrium concentration of Na_{Li} is 1 % at 1100 K, whereas that of Na_{Co} is 10^{-11}. This indicates that Na preferentially substitutes for Li in $LiCoO_2$. Since Na is monovalent the same as Li, Na doping has little effect on the concentrations of the native defects in $LiCoO_2$. Figure 6(c) illustrates the equilibrium defect concentrations at condition B. Na chemical potential is higher and Li chemical potential is lower than at condition A, and thus the equilibrium concentration of Na_{Li} becomes increased to be about 4 % at 1100 K. The lower Li chemical potential causes increases in the native defects. But the actual increase is insignificant because of the small differences in the chemical potentials, as shown in Fig. 6(a).

It is reported that K and Rb form oxides of Li*M*O and $MCoO_2$ (*M* = K and Rb). The present calculations show lower energy for the combination of Li_2O and $MCoO_2$ than that for $LiCoO_2$ and Li*M*O. Therefore, defect concentrations for K and Rb-doped $LiCoO_2$ are estimated at the coexistence conditions with Li_2O and $MCoO_2$. The defect concentrations of K and Rb are 10^{-15} or less at 1100 K for both the Li and Co sites. This indicates that both K and Rb are insoluble in $LiCoO_2$.

Doping of divalent metals: Mg, Ca, Sr and Zn

Mg does not form complex oxides with Li. Therefore, the maximum Li chemical potential is compatible with the maximum Mg one in the stability region of $LiCoO_2$, as illustrated in Fig. 7(a) at 1100 K. Figure 7(b) illustrates equilibrium defect concentrations in Mg-doped $LiCoO_2$ at condition A in Fig. 7(a), where $LiCoO_2$ coexists with Li_2O and MgO. This condition corresponds to the maximum chemical potentials of both Li and Mg. The equilibrium defect concentrations of both Mg_{Li} and Mg_{Co} are about 0.5 % at 1100 K with small temperature dependence, indicating that Mg can substitute for both Li and Co. As Mg is a divalent species different from either Li or Co in $LiCoO_2$, two charge states are considered for each substitution for the Li and Co sites; one is a single Mg ion having a relative charge (Mg_{Li}^{+} and Mg_{Co}^{-}), and the other is a Mg ion coupled with an electronic defect of a small polaron ($[Mg_{Li} + e]^0$ and $[Mg_{Co} + h]^0$). At the present condition, the single Mg ions without electronic defects are predominant for both the Li and Co sites. The charge neutrality of the Mg doping is predominantly kept by the simultaneous Mg substitution for both the Li and Co sites, and secondary by compensational change in the concentrations of e^- and Co_{Li}^{+}. Mg is, therefore, amphibious in $LiCoO_2$ in terms of the relative charge and also of the occupation site. This suggests that the preferential occupation site of Mg depends on the synthetic condition. To evaluate the tendency under more oxidative conditions, O chemical potential is simply set higher by 0.5 eV than condition A in Fig. 7(a), and equilibrium defect concentrations are estimated as illustrated in Fig. 7(c). The oxidative condition suppresses Mg_{Li}^{+}, Co_{Li}^{+}, V_O^0 and e^-, and increases Mg_{Co}^{-} and h^+. Mg is often supposed to substitute for the Co site as $Li(Mg_xCo_{1-x})O_2$,[1,8,10] but Mladenov *et al.* suggested that Mg substituted for both the Li and Co sites as $(Mg_yLi_{1-y})(Mg_xCo_{1-x})O_2$ from X-ray diffraction (XRD) measurements and Rietveld analysis.[22] Moreover, in the case of $LiNiO_2$, Mg is reported to substitute for both Li and Ni.[7] The simultaneous occupation suggested in the present calculation is consistent with the later reports. There are contrary opinions on the role of the Mg ions in the Li layers. Pouillerie *et al.* reported that the Mg ions in the Li layers prevent the local collapses of the structure for Mg-doped $LiNiO_2$, resulting in good cycling stability.[7] In contrast, Mladenov *et al.* reported that the Mg ions in the Co layers in $LiCoO_2$ have a positive effect on the cycling stability, while those in the Li layers do not influence the capacity fade.[22] Although the role of the doped Mg ions is beyond the scope of this study, one can know appropriate conditions for the doping to the individual sites; the oxidative conditions are desirable for Mg_{Co}, whereas the reductive conditions are better for Mg_{Li}.

Neither Ca nor Sr forms complex oxides with Li, as similar to Mg. Therefore, equilibrium defect concentrations in Ca and Sr-doped $LiCoO_2$ are evaluated at the conditions where $LiCoO_2$ coexists with Li_2O and *M*O (*M* = Ca and Sr). The concentration of Ca_{Li} is 10^{-6} at 1100 K, whereas that of Ca_{Co} is 10^{-11}. The concentrations of Sr_{Li} and Sr_{Co} are less than 10^{-11}. These results indicate that Ca and Sr are both insoluble to $LiCoO_2$.

In contrast to Mg and alkaline-earth metals, Zn forms complex oxides with Li. The present calculations find that Li_6ZnO_4 and $Li_{10}Zn_4O_9$ can coexist with $LiCoO_2$. The stability region of $LiCoO_2$ projected on a space of Li and Zn chemical potentials is illustrated in Fig. 8(a). Figures 8(b) illustrates the equilibrium defect concentrations when $LiCoO_2$ coexists with Li_2O and Li_6ZnO_4, which is denoted by condition A in Fig. 8(a). The concentration of Zn_{Li} is estimated to be 60 % at 1100 K with small temperature dependence. The concentration of Zn_{Co} is as low as 10^{-7}. Under higher Zn chemical potential, *e.g.*, when $LiCoO_2$ coexists with Li_6ZnO_4 and $Li_{10}Zn_4O_9$ as denoted by condition B in Fig. 8(a), the concentration of Zn_{Li} becomes close to 100 %. These results suggest that Zn is highly soluble to the Li site in $LiCoO_2$. The doped Zn ion is mainly coupled with a neighboring small polaron of electron as $[Zn_{Li} + e]^0$. Since the relative charge of the Zn ion is cancelled by the coupled electron, the Zn doping has only a small effect on the concentrations of the native defects in $LiCoO_2$. Although the surface coating of ZnO is often applied to $LiCoO_2$, the present calculation results suggest that ZnO can react with $LiCoO_2$ during the coating processes, leading to the unexpected doping of Zn and the formation of Li–Zn oxides. The presence of Li_6ZnO_4 in the coating film of the ZnO-coated $LiCoO_2$ particles is observed by the transmission electron microscopy (TEM) and the selected area diffraction (SAD) pattern measurements.[25] The improved thermal stability by the ZnO coating[27] may be a positive effect of Zn_{Li} that can prevent the collapse of the layered structure.

Doping of Zr and Nb

Zr forms complex oxides of Li_2ZrO_3 and $Li_6Zr_2O_7$. Figure 9(a) illustrates the stability region of $LiCoO_2$ in Li and Zr chemical potentials. Equilibrium defect concentrations are estimated at the conditions where $LiCoO_2$ coexists with Li_2O and $Li_6Zr_2O_7$ as denoted by condition A in Fig. 9(a), *i.e.*, the maximum Li chemical potential, with $Li_6Zr_2O_7$ and Li_2ZrO_3 of condition B, and with Li_2ZrO_3 and ZrO_2 of condition C, *i.e.*, the maximum Zr chemical potential. Figure 9(b) illustrates the equilibrium defect concentrations at condition C. Even though Zr chemical potential is the maximum, the concentrations of Zr_{Li} and Zr_{Co} are respectively 10^{-8} and 10^{-6} at 1100 K. This suggests that Zr is

insoluble to $LiCoO_2$. Luo and Dahn reported that $Li(Zr_xCo_{1-x})O_2$ cannot be prepared even for additions of Zr as low as 1 % with the careful characterization of the synthesis and structure.[13] The present calculation results are in good agreement with their results. The high Zr chemical potential at condition C leads to low Li chemical potential, increasing the lithium-deficient defects, *i.e.*, Co_{Li} and V_{Li}. To reduce the lithium deficiency, say the concentration of Co_{Li} less than 1 %, sufficiently excess Li and high Li chemical potential like condition A are necessary, although the Zr solubility becomes as low as 10^{-8}. ZrO_2 is often used for the surface coating of electrode active materials.[23,28] The present calculation results suggest that the surface of $LiCoO_2$ could be exposed to low Li chemical potential during the heat-treatment processes, and this could generate the lithium-deficient defects near the surface.

Nb forms complex oxides such as $LiNbO_3$ and Li_3NbO_4. Thus, the equilibrium defect concentrations are estimated at the conditions where $LiCoO_2$ coexists with Li_2O and Li_3NbO_4, and with Li_3NbO_4 and $LiNbO_3$. At the former condition with the maximum Li chemical potential, the concentrations of Nb_{Li} and Nb_{Co} are respectively 10^{-16} and 10^{-9}. Even at the more Nb-rich condition of the coexistence with Li_3NbO_4 and $LiNbO_3$, the concentration of Nb_{Co} is 10^{-4}, although the concentration of Co_{Li} becomes almost 100 %. These results indicate that Nb is insoluble to $LiCoO_2$.

Factors for occupation sites and solubility limits

The occupation sites and solubility limits of the dopants are the principal information to control the doping. However, our calculation demonstrates that dopants that can be experimentally detectable, say the solubility limit is 1 % or higher, are very limited; Al and Ga at the Co site, Na and Zn at the Li site, and Mg as the total of both the sites at 1100 K without significant increase in the lithium-deficient defects, Co_{Li} in particular. Furthermore, experimental determination on whether the dopants are soluble or insoluble is generally based on observation of other phases. Thus, one has difficulty of the determination, particularly with low solubility, leading to limited and qualitative information on the doping. On the other hand, the present calculation can provide the dopant solubility quantitatively for each individual site, even when the solubility is very low. Therefore, properties of the dopants and their solubility are herein discussed based on the calculation results. Since the dopant solubility depends on the chemical potentials, the estimation at the following conditions is used. Three-phase coexistence conditions, *i.e.*, $LiCoO_2$ with $Li_3Na_2CoO_4$ and $NaCoO_2$, Li_2O and $MCoO_2$ (M = K and Rb), Li_2O and MO (M = Mg, Ca and Sr), Li_2O and Li_6ZnO_4, Li_5MO_4 and $LiMO_2$ (M = Al and Ga), Li_2O and $LiMO_2$ (M = Sc, In and Y), Li_2O and $Li_6Zr_2O_7$, and Li_2O and Li_3NbO_4, are selected at a temperature of 1100 K. Most of these conditions correspond to the maximum Li chemical potential to suppress the concentration of Co_{Li} to be less than 1 %. Al, Ga and Na are exceptions, and the best conditions are chosen for these dopants in terms of the balance of the increase in the dopant solubility and the suppression of the lithium deficiency, as already discussed.

Figure 10(a) illustrates the dopant solubility at the Li and Co sites sorted by the valence of the dopants. Figure 10(b) shows the same solubility as a function of six-coordinate ionic radii of the dopants.[52] It is clear that monovalent and divalent dopants show higher concentration of M_{Li} than that of M_{Co}. On the other hand, trivalent and higher-valent dopants show higher concentration of M_{Co} than that of M_{Li}. These results indicate that the valences of the dopants are the predominant factor for the preferential occupation sites, suggesting that electrostatic interaction among the defects by the relative charges is significant. Comparing the solubility among the dopants having the same valence, closer ionic radius to Li leads to higher solubility of M_{Li}, and closer radius to Co leads to higher solubility of M_{Co}. Larger difference in the ionic radius shows lower solubility. Although the predominant factor for the occupation sites is the valence, the ionic radius difference also has a significant effect on the dopant solubility. The divalent dopants have the relative charges of +1 for M_{Li} and –1 for M_{Co}, and thus these two are equivalent in terms of the relative charges. Since the divalent dopants examined in this study have closer ionic radii to Li than Co, they show higher solubility of M_{Li}.

Conclusions

The defect formation energy and concentration under thermal equilibrium are evaluated for the doped ions and native defects in $LiCoO_2$ based on the first-principles DFT calculations. Na, K, Rb, Mg, Ca, Sr, Zn, Al, Ga, In, Sc, Y, Zr and Nb are examined as the dopants. Al and Ga show the solubility of 1 % or higher at the Co site at 1100 K without significant increase in the lithium-deficient deficiency, and Na and Zn show the solubility of 1 % or higher at the Li site. Mg shows the solubility of about 0.5 % at both the Li and Co sites, and its preferential occupation site depends on the synthetic conditions. The oxidative conditions are desirable for the doping to the Co site, whereas the reductive conditions are better to the Li site. The solubility of other dopants is 0.1 % or less, or the lithium deficiency becomes significant. The estimated solubility indicates that the valences of the dopants are the predominant factor for the occupation sites: the Li site for monovalent and divalent dopants, and the Co site for trivalent and higher-valent dopants. The ionic radii of the doped ions have a significant effect on the solubility: closer radii to Li and Co lead to higher solubility to the Li and Co sites, respectively. Larger difference in the ionic radius results in lower solubility.

The dopant solubility and the defect concentrations strongly depend on the conditions. Even for Al, which is well known to be highly soluble to $LiCoO_2$, too high Li chemical potential suppresses the Al solution, and too high Al chemical potential increases the lithium deficiency. To achieve the balance of the high dopant solubility and the low lithium deficiency, appropriate ratio of the starting materials that provides the desirable chemical potentials is necessary. The present scheme based on the first-principles calculations can provide quantitative information about the balance of the defects and also about the proper conditions. This information is valuable not only for designing the synthetic processes but also for judging the appropriateness of the post-synthetic processes, *e.g.*, the heat treatment for the surface modification.

Acknowledgement

This work was supported by the Research and Development Initiative for Scientific Innovation of New Generation Battery

(RISING) project from New Energy and Industrial Technology Development Organization (NEDO), Japan.

Notes and references

[a] *Office of Society-Academia Collaboration for Innovation, Kyoto University, Gokasho, Uji, Kyoto 611-0011, Japan. E-mail: koyama@saci.kyoto-u.ac.jp*
[b] *Department of Materials Science and Engineering, Graduate School of Engineering, Kyoto University, Yoshida, Sakyo, Kyoto 606-8501, Japan*
[c] *Graduate School of Human and Environment Studies, Kyoto University, Yoshida Nihon-matsu, Sakyo, Kyoto 606-8501, Japan*

1. H. Tukamoto and A. R. West, *J. Electrochem. Soc.*, 1997, **144**, 3164-3168.
2. Y. I. Jang, B. Y. Huang, Y. M. Chiang and D. R. Sadoway, *Electrochem. Solid State Lett.*, 1998, **1**, 13-16.
3. S. T. Myung, N. Kumagai, S. Komaba and H. T. Chung, *Solid State Ionics*, 2001, **139**, 47-56.
4. A. D'Epifanio, F. Croce, F. Ronci, V. Rossi Albertini, E. Traversa and B. Scrosati, *Phys. Chem. Chem. Phys.*, 2001, **3**, 4399-4403.
5. R. Stoyanova, E. Zhecheva, G. Bromiley, T. B. Ballaran, R. Alcántara, J. I. Corredor and J. L. Tirado, *J. Mater. Chem.*, 2002, **12**, 2501-2506.
6. D. G. Tong, Y. Y. Luo, Y. He, X. Y. Ji, J. L. Cao, L. X. Tang, A. D. Tang, K. L. Huang and Q. Y. Lai, *Mater. Sci. Eng. B-Solid State Mater. Adv. Technol.*, 2006, **128**, 220-228.
7. C. Pouillerie, L. Croguennec, Ph. Biensan, P. Willmann and C. Delmas, *J. Electrochem. Soc.*, 2000, **147**, 2061-2069.
8. S. Levasseur, M. Ménétrier and C. Delmas, *Chem. Mater.*, 2002, **14**, 3584-3590.
9. H. S. Kim, T. K. Ko, B. K. Na, W. I. Cho and B. W. Chao, *J. Power Sources*, 2004, **138**, 232-239.
10. W. Luo, X. Li and J. R. Dahn, *J. Electrochem. Soc.*, 2010, **157**, A782-A790.
11. S. H. Kim and C. S. Kim, *J. Electroceram.*, 2009, **23**, 254-257.
12. S. A. Needham, G. X. Wang, H. K. Liu, V. A. Drozd and R. S. Liu, *J. Power Sources*, 2007, **174**, 828-831.
13. W. B. Luo and J. R. Dahn, *J. Electrochem. Soc.*, 2011, **158**, A110-A114.
14. J. Bludská, J. Vondrák, P. Stopka and I. Jakubec, *J. Power Sources*, 1992, **39**, 313-322.
15. M. Holzapfel, C. Darie, P. Bordet, E. Chappel, M. D. Núnez-Regueiro, S. Diaz, S. de Brion, G. Chouteau and P. Strobel, *Solid State Sci.*, 2005, **7**, 497-506.
16. J. M. Tarascon, F. Coowar, G. Amatuci, F. K. Shokoohi and D. G. Guyomard, *J. Power Sources*, 1995, **54**, 103-108.
17. H. Arai, S. Okada, H. Ohtsuka, M. Ichimura and J. Yamaki, *Solid State Ionics*, 1995, **80**, 261-269.
18. A. Rougier, P. Gravereau and C. Delmas, *J. Electrochem. Soc.*, 1996, **143**, 1168-1175.
19. Y. Y. Xia and M. Yoshio, *J. Electrochem. Soc.*, 1997, **144**, 4186-4194.
20. R. Amin and J. Maier, *Solid State Ionics*, 2008, **178**, 1831-1836.
21. H. J. Kweon, S. J. Kim and D. G. Park, *J. Power Sources*, 2000, **88**, 255-261.
22. M. Mladenov, R. Stoyanova, E. Zhecheva and S. Vassilev, *Electrochem. Commun.*, 2001, **3**, 410-416.
23. J. Cho, Y. J. Kim, T. J. Kim and B. Park, *Angew. Chem.-Int. Edit.*, 2001, **40**, 3367-3369.
24. Y. Iriyama, H. Kurita, I. Yamada, T. Abe and Z. Ogumi, *J. Power Sources*, 2004, **137**, 111-116.
25. T. Fang, J. G. Duh and S. R. Sheen, *J. Electrochem. Soc.*, 2005, **152**, A1701-A1706.
26. L. Dahéron, R. Dedryvère, H. Martinez, D. Flahaut, M. Ménétrier, C. Delmas and D. Gonbeau, *Chem. Mater.*, 2009, **21**, 5607-5616.
27. W. Chang, J. W. Choi, J. C. Im and J. K. Lee, *J. Power Sources*, 2010, **195**, 320-326.
28. Z. H. Chen, Y. Qin, K. Amine and Y. K. Sun, *J. Mater. Chem.*, 2010, **20**, 7606-7612, and references therein.
29. G. Ceder and S. K. Mishra, *Electrochem. Solid State Lett.*, 1999, **2**, 550-552.
30. S. Buta, D. Morgan, A. Van der Ven, M. K. Aydinol and G. Ceder, *J. Electrochem. Soc.*, 1999, **146**, 4335-4338.
31. S. Q. Shi, D. S. Wang, S. Meng, L. Q. Chen and X. J. Huang, *Phys. Rev. B*, 2003, **67**, 115130.
32. T. Amriou, A. Sayede, B. Khelifa, C. Mathieu and H. Aourag, *J. Power Sources*, 2004, **130**, 213-220.
33. Y. Koyama, Y. Makimura, I. Tanaka, H. Adachi and T. Ohzuku, *J. Electrochem. Soc.*, 2004, **151**, A1499-A1506.
34. O. Clemens, M. Bauer, R. Haberkorn, M. Springborg and H. P. Beck, *Chem. Mater.*, 2012, **24**, 4717-4724.
35. X. Ma, G. Hautier, A. Jain, R. Doe and G. Ceder, *J. Electrochem. Soc.*, 2013, **160**, A279-A284.
36. C. Y. Ouyang, S. Q. Shi, Z. X. Wang, H. Li, X. J. Huang and L. Q. Chen, *J. Phys.-Condes. Matter*, 2004, **16**, 2265-2272.
37. M. V. Koudriachova and N. M. Harrison, *J. Mater. Chem.*, 2006, **16**, 1973-1977.
38. A. Dianat, N. Seriani, M. Bobeth and G. Cuniberti, *J. Mater. Chem. A*, 2013, **1**, 9273-9280.
39. K. Hoang and M. D. Johannes, *J. Power Sources*, 2012, **206**, 274-281.
40. Y. Koyama, H. Arai, I. Tanaka, Y. Uchimoto and Z. Ogumi, *Chem. Mater.*, 2012, **24**, 3886-3894.
41. Y. Koyama, H. Arai, I. Tanaka, Y. Uchimoto and Z. Ogumi, *J. Power Sources*, 2013, **244**, 592-596.
42. R. Koksbang, J. Barker, H. Shi and M. Y. Saïdi, *Solid State Ionics*, 1996, **84**, 1-21.
43. M. W. Chase, Jr. and National Institute of Standards and Technology, *NIST-JANAF Thermochemical Tables*, American Institute of Physiscs, Woodbury, 4th edn., 1998, pp. 1745.
44. S. Pöykkö, M. J. Puska and R. M. Nieminen, *Phys. Rev. B*, 1996, **53**, 3813-3819.
45. C. G. Van de Walle and J. Neugebauer, *J. Appl. Phys.*, 2004, **95**, 3851-3879.
46. K. Hoang and M. Johannes, *Chem. Mater.*, 2011, **23**, 3003-3013.
47. G. Kresse and J. Furthmüller, *Phys. Rev. B*, 1996, **54**, 11169-11186.
48. P. E. Blöchl, *Phys. Rev. B*, 1994, **50**, 17953-17979.
49. G. Kresse and D. Joubert, *Phys. Rev. B*, 1999, **59**, 1758-1775.
50. J. P. Perdew, K. Burke and M. Ernzerhof, *Phys. Rev. Lett.*, 1996, **77**, 3865-3868.
51. S. L. Dudarev, G. A. Botton, S. Y. Savrasov, C. J. Humphreys and A. P. Sutton, *Phys. Rev. B*, 1998, **57**, 1505-1509.
52. R. D. Shannon, *Acta Crystallogr., Sect. A*, 1976, **32**, 751-767.

Figure caption:

Fig. 1 Stability region of Al-doped $LiCoO_2$ in Li and Al chemical potentials at 1100 K with limits imposed by competing phases.

Fig. 2 Defect formation energies in Al-doped $LiCoO_2$ as a function of Fermi energy when $LiCoO_2$ coexists with (a) Li_2O and Li_5AlO_4 (condition A in Fig. 1) at 1100 K, (b) Li_5AlO_4 and $LiAlO_2$ (B in Fig. 1), and (c) $LiAlO_2$ and $CoAl_2O_4$ (C in Fig. 1), respectively.

Fig. 3 Defect formation energies in Al-doped $LiCoO_2$ and chemical potentials of Li, Co and Al along conditions X–A–B–C–Y in Fig. 1 under the charge neutral condition at 1100 K.

Fig. 4 Equilibrium defect concentrations in Al-doped $LiCoO_2$ as a function of temperature, when $LiCoO_2$ coexists with (a) Li_2O and Li_5AlO_4 (condition A in Fig. 1), (b) Li_5AlO_4 and $LiAlO_2$ (B in Fig. 1), and (c) $LiAlO_2$ and $CoAl_2O_4$ (C in Fig. 1), respectively. (d) Equilibrium defect concentrations in undoped $LiCoO_2$ coexisting with Li_2O. The concentrations are given both per the formula unit (in $f.u.^{-1}$) and per volume (in cm^{-3}).

Fig. 5 Equilibrium defect concentrations as a function of temperature in (a) Ga-doped $LiCoO_2$ coexisting with Li_5GaO_4 and $LiGaO_2$, and (b) Sc-doped $LiCoO_2$ coexisting with Li_2O and $LiScO_2$, respectively.

Fig. 6 (a) Stability region of Na-doped $LiCoO_2$ in Li and Na chemical potentials at 1100 K with limits imposed by competing phases. Equilibrium defect concentrations in Na-doped $LiCoO_2$ as a function of temperature, when $LiCoO_2$ coexists with (b) Li_2O and $Li_3Na_2CoO_4$ (condition A), and (c) $Li_3Na_2CoO_4$ and $NaCoO_2$ (condition B), respectively.

Fig. 7 (a) Stability region of Mg-doped $LiCoO_2$ in Li and Mg chemical potentials at 1100 K with limits imposed by competing phases. (b) Equilibrium defect concentrations in Mg-doped $LiCoO_2$ as a function of temperature when $LiCoO_2$ coexists with Li_2O and MgO (condition A), and (c) those under oxidative condition by 0.5 eV in O chemical potential.

Fig. 8 (a) Stability region of Zn-doped $LiCoO_2$ in Li and Zn chemical potentials at 1100 K with limits imposed by competing phases. (b) Equilibrium defect concentrations in Zn-doped $LiCoO_2$ as a function of temperature when $LiCoO_2$ coexists with Li_2O and Li_6ZnO_4 (condition A).

Fig. 9 (a) Stability region of Zr-doped $LiCoO_2$ in Li and Zr chemical potentials at 1100 K with limits imposed by competing phases. (b) Equilibrium defect concentrations in Zr-doped $LiCoO_2$ as a function of temperature when $LiCoO_2$ coexists with Li_2ZrO_3 and ZrO_2 (condition C).

Fig. 10 Dopant solubility at the Li and Co sites in $LiCoO_2$ at 1100 K (a) sorted by the valence of the dopants, and (b) illustrated as a function of ionic radius, respectively. Broken lines in panel (b) denote ionic radii of Li^+ and Co^{3+}(LS).

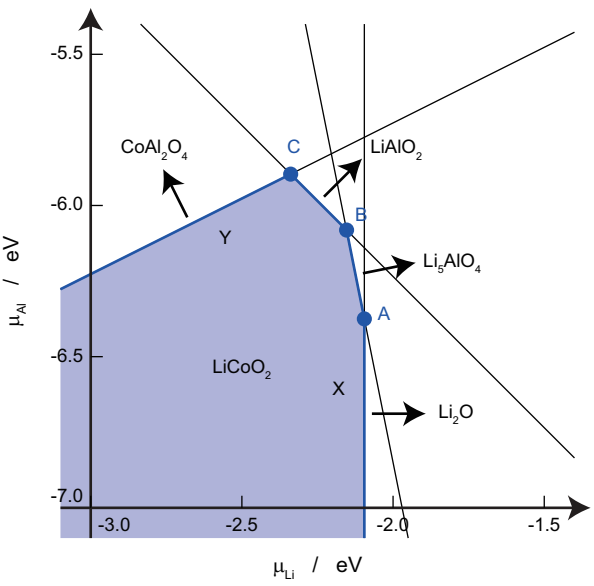
-5.5
-6.0
-6.5
-7.0
-3.0
-2.5
-2.0
-1.5
μ_{Al} / eV
μ_{Li} / eV
$CoAl_2O_4$
C
$LiAlO_2$
B
Y
Li_5AlO_4
A
$LiCoO_2$
X
Li_2O

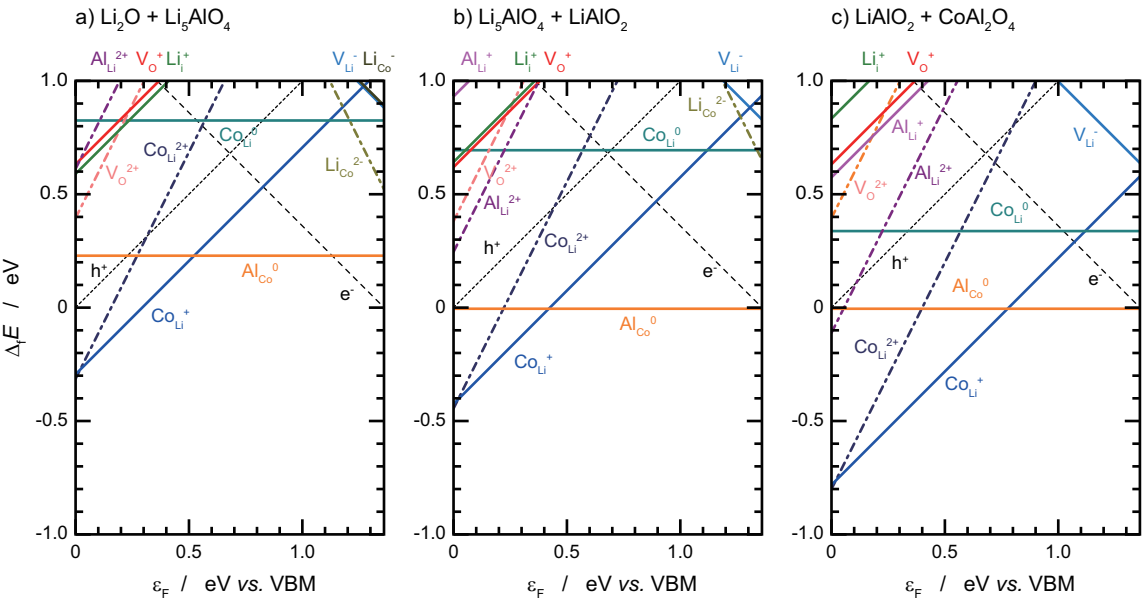
a) Li2O + Li5AlO4
b) Li5AlO4 + LiAlO2
c) LiAlO2 + CoAl2O4
ΔfE / eV
εF / eV vs. VBM
h+
e-
VO2+
VO+
Li+i
VLi-
LiCo2-
CoLi0
CoLi2+
CoLi+
AlCo0
AlLi2+
AlLi+
1.0
0.5
0
-0.5
-1.0
0
0.5
1.0

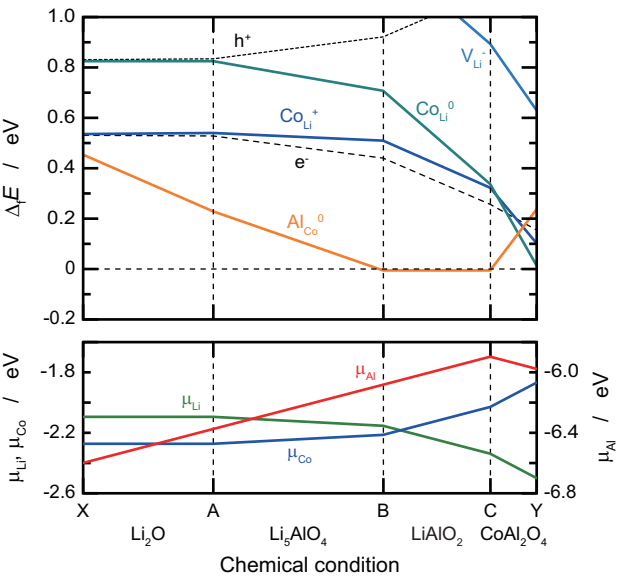
1.0
0.8
0.6
0.4
0.2
0
-0.2
ΔfE / eV
h+
V_Li -1
Co_Li +
Co_Li 0
e-
Al_Co 0
-1.8
-2.2
-2.6
μLi, μCo / eV
μAl
μLi
μCo
-6.0
-6.4
-6.8
μAl / eV
X
A
B
C
Y
Li2O
Li5AlO4
LiAlO2
CoAl2O4
Chemical condition

a) Al-doped $LiCoO_2$ with Li_2O + Li_5AlO_4

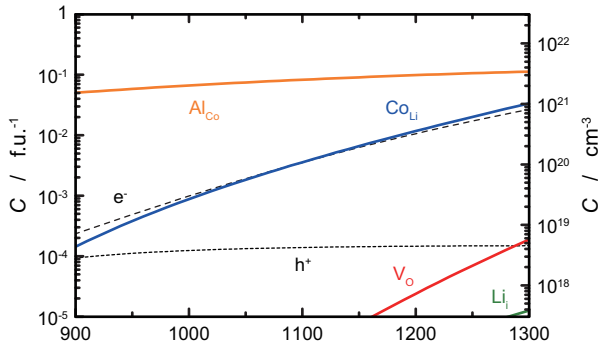

b) Al-doped $LiCoO_2$ with Li_5AlO_4 + $LiAlO_2$

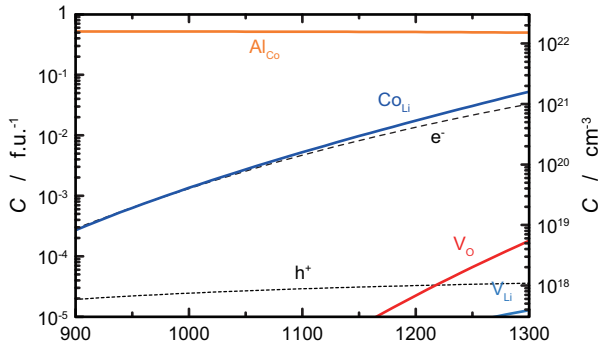

c) Al-doped $LiCoO_2$ with $LiAlO_2$ + $CoAl_2O_4$

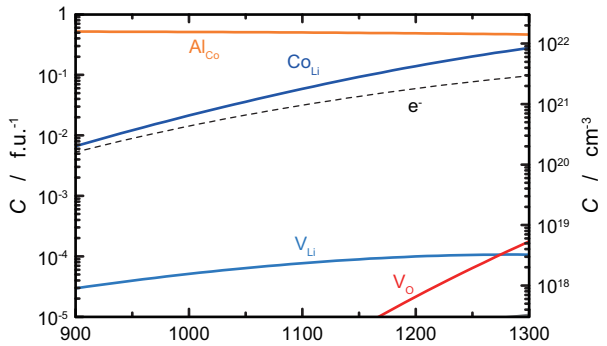

d) Undoped $LiCoO_2$ with Li_2O

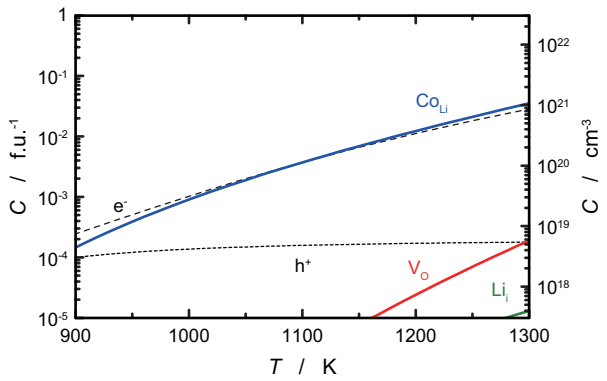

a) Ga-doped $LiCoO_2$ with Li_5GaO_4 + $LiGaO_2$

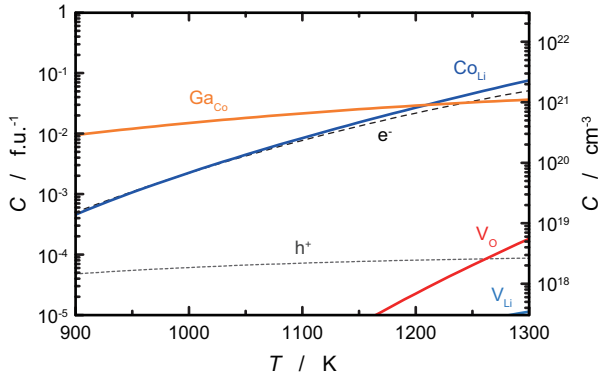

b) Sc-doped $LiCoO_2$ with Li_2O + $LiScO_2$

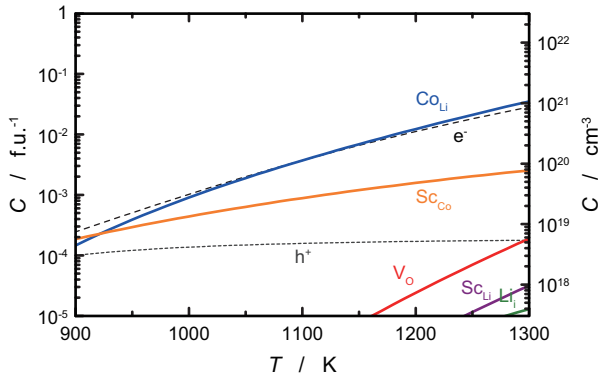

a)

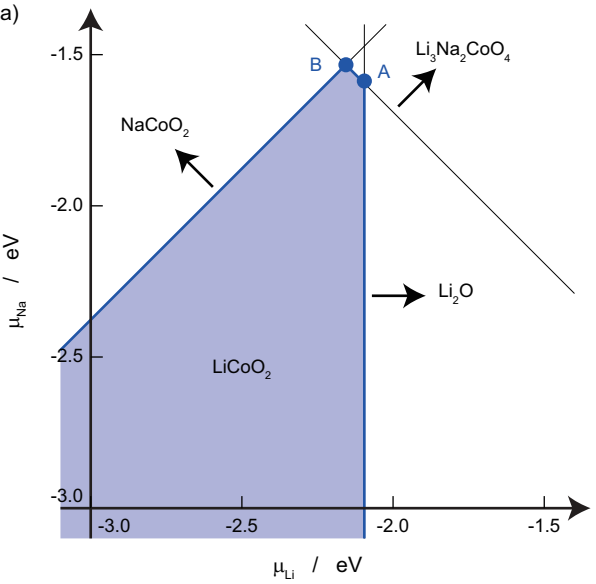

b) Na-doped $LiCoO_2$ with Li_2O + $Li_3Na_2CoO_4$

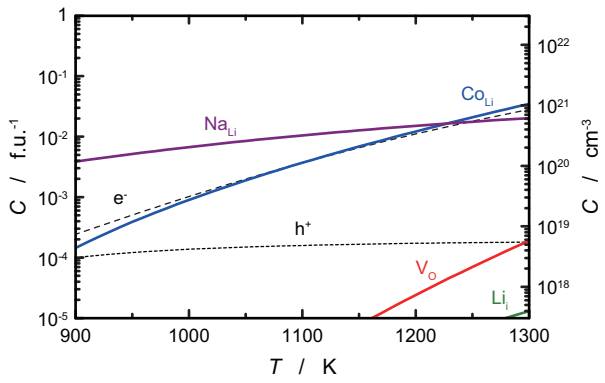

c) Na-doped $LiCoO_2$ with $Li_3Na_2CoO_4$ + $NaCoO_2$

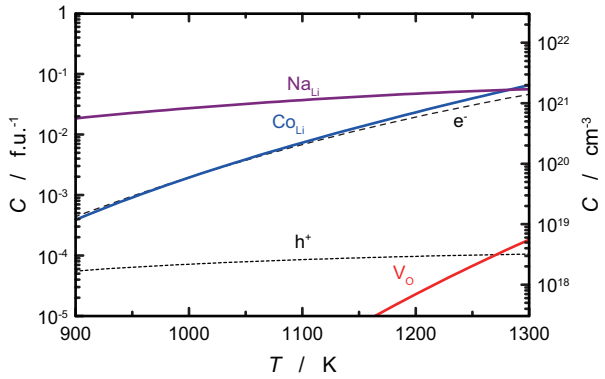

a)

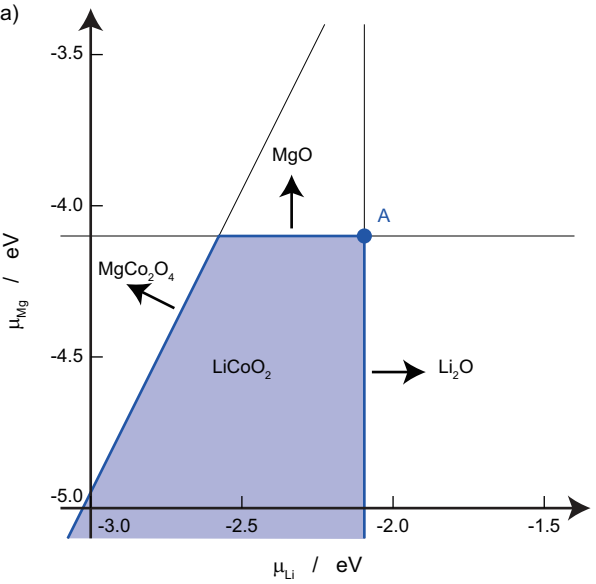

b) Mg-doped $LiCoO_2$ with Li_2O + MgO

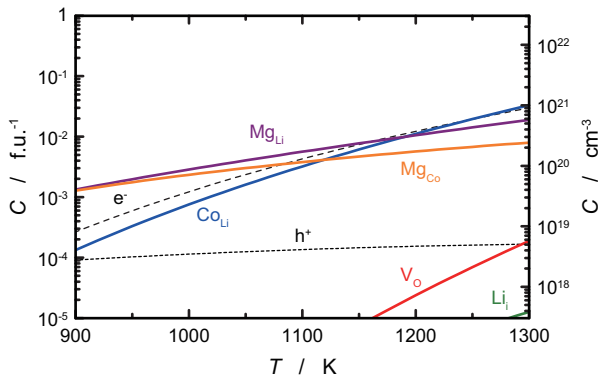

c) Mg-doped $LiCoO_2$ under oxidative condition

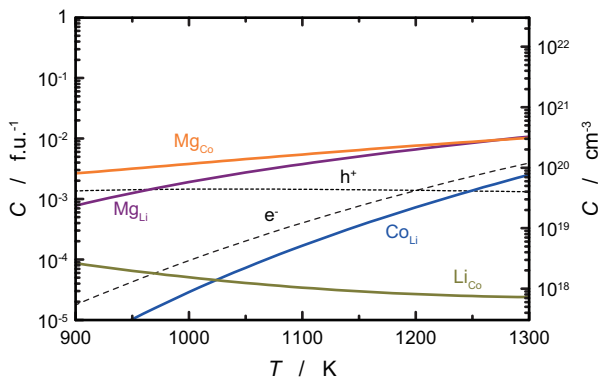

a)

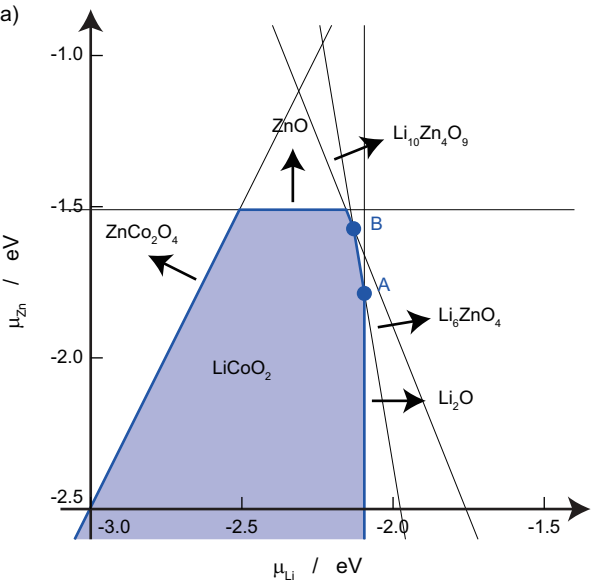

b) Zn-doped $LiCoO_2$ with Li_2O + Li_6ZnO_4

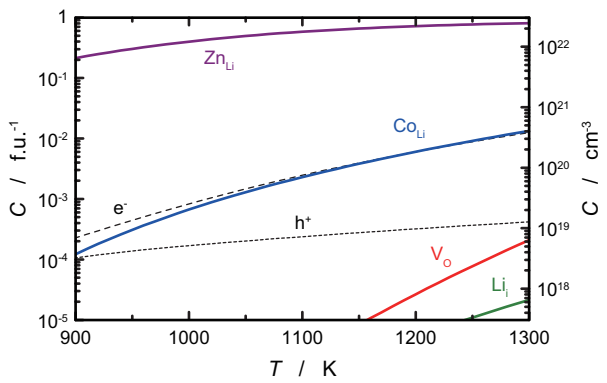

a)

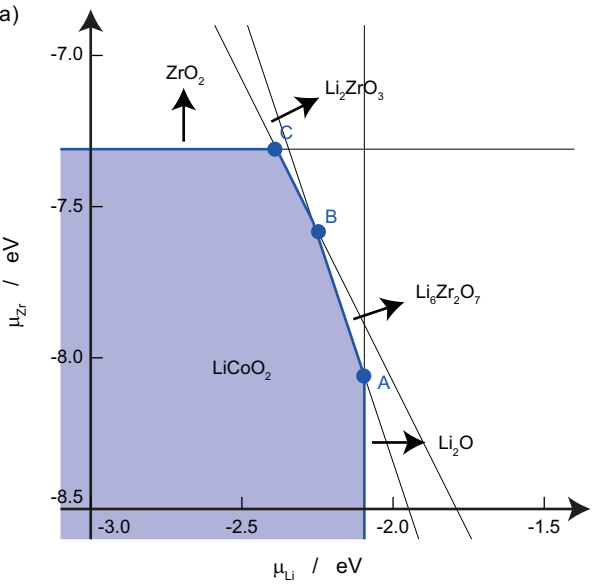

b) Zr-doped $LiCoO_2$ with Li_2ZrO_3 + ZrO_2

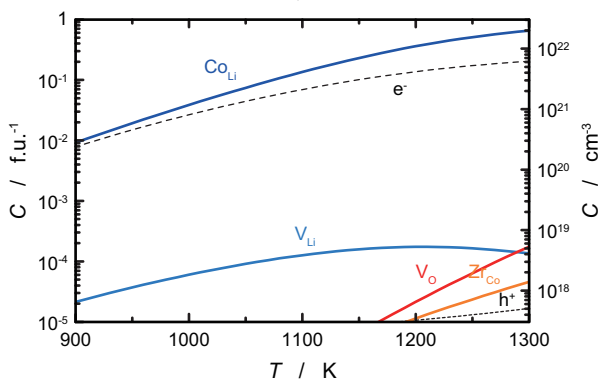

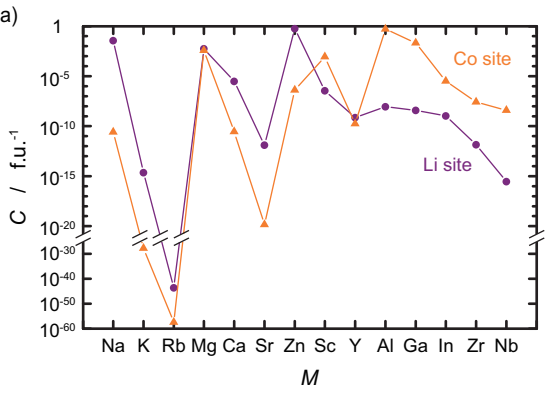
a)
1
10-5
10-10
10-15
10-20
10-30
10-40
10-50
10-60
C / f.u.-1
Co site
Li site
Na K Rb Mg Ca Sr Zn Sc Y Al Ga In Zr Nb
M

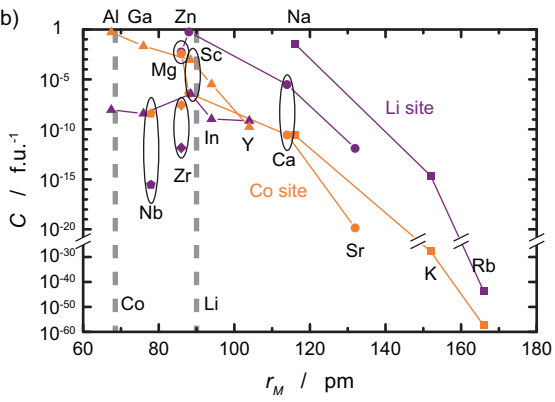
b)
Al Ga Zn
Na
Mg
Sc
In
Y
Ca
Zr
Nb
Li site
Co site
Sr
K
Rb
Co
Li
1
10-5
10-10
10-15
10-20
10-30
10-40
10-50
10-60
C / f.u.-1
60 80 100 120 140 160 180
rM / pm

Graphical abstract

First-principles study of doped ions in $LiCoO_2$ provides guidelines for synthetic and post-synthetic conditions to balance dopant solubility and suppression of native defects.